inantly small-angle collisions.[14-16] For such normal-process collisions, second sound cannot be expected to occur, and, in fact, no indication of second sound or even of an approach to second sound is seen in the data.

The data for both the 0.4-in. diameter and the 0.1-in. diameter heat source show no essential difference. The larger heat source would be the more likely one for which second sound might be observed. The ratios of input pulse width to transit times in the $\frac{1}{2}$-cm crystal were ~0.1 and 0.05 for the longitudinal and transverse pulses, respectively. Thus most of the external conditions for this experiment were rather similar to those employed in the recent experiment on solid helium for which the observation of second sound has been reported.[4] Even though there is not necessarily a direct conflict between these two results (since the role of phonon collisions may be quite different in the two materials), it would be of considerable interest to extend the solid-helium results to lower temperatures to investigate the transition from the reported behavior to the expected ballistic flow at the ordinary sound velocity.

*Partially supported by U. S. Army Electronics Command, Fort Monmouth, New Jersey, under Contract No. DA36-039 AMC-02280(E).

[1]R. J. von Gutfeld and A. H. Nethercot, Phys. Rev. Letters 12, 641 (1964).
[2]J. M. Andrews and M. W. P. Strandberg, Proc. IEEE 54, 523 (1966).
[3]J. B. Brown, D. Y. Chung, and P. W. Matthews, Phys. Letters 21, 241 (1966).
[4]C. C. Ackerman, B. Bertram, H. A. Fairbank, and R. A. Guyer, Phys. Rev. Letters 16, 789 (1966).
[5]R. J. von Gutfeld and A. H. Nethercot, in Proceedings of the Ninth International Conference on Low-Temperature Physics (Plenum Press, New York, 1965), pp. 1189-1192.
[6]J. C. Ward and J. Wilks, Phil. Mag. 42, 314 (1951).
[7]R. A. Guyer and J. A. Krumhansl, Phys. Rev. 148, 778 (1966).
[8]R. Berman, Z. Physik. Chem. (Frankfurt) 16, 10 (1958).
[9]R. J. von Gutfeld, A. H. Nethercot, Jr., and J. A. Armstrong, Phys. Rev. 142, 436 (1965).
[10]R. J. von Gutfeld and A. H. Nethercot, Jr., J. Appl. Phys. 37, 3767 (1966).
[11]G. W. Farnell, Can. J. Phys. 39, 65 (1961).
[12]J. de Klerk, Phys. Rev. 139, A1635 (1965).
[13]H. G. Carslaw and J. C. Jaeger, Conduction of Heat in Solids, Clarendon Press, Oxford, England, 1947, p. 57.
[14]S. Simons, Proc. Phys. Soc. (London) 82, 401 (1963).
[15]H. J. Maris, Phil. Mag. 9, 901 (1964).
[16]I. S. Ciccarello and K. Dransfeld, Phys. Rev. 134, A1517 (1964).

de HAAS-van ALPHEN EFFECT IN FERROMAGNETIC NICKEL*

D. C. Tsui† and R. W. Stark‡
Department of Physics and Institute for the Study of Metals, The University of Chicago, Chicago, Illinois
(Received 8 September 1966)

We report here an investigation of the de Haas–van Alphen effect in nickel. The results are discussed in terms of the models which have been recently proposed for the band structure of ferromagnetic nickel.

We wish to report in this Letter the preliminary results of our de Haas–van Alphen (dHvA) investigation of the Fermi surface of nickel. Several models have recently been proposed for the ferromagnetic nickel band structure.[1-5] In general, these models are quite similar in their gross features but differ in detail. This similarity is expected since rather stringent limitations are placed on any proposed model. The exchange interactions are small compared with the crystal potential so that one assumes that the ferromagnetic band structure can be obtained from the paramagnetic band structure[6,7] by considering the exchange splitting as a perturbation. In addition, the resulting model must meet the dual criteria of having an excess of about 0.55 spin-up ($\uparrow$) electrons[8] and a Fermi surface enclosing a net volume corresponding to one electron per atom.[9] It must also have one open sheet, similar to the copper Fermi surface, to satisfy the magnetoresistance experiments of Fawcett and Reed[10] and the dHvA experiments of Joseph and Thorsen (JT).[11] The dHvA data which we present here offer the first independent confirmation of this general approach to the ferromagnetic nickel band structure.

The single-crystal nickel samples which were used in this experiment were prepared by electron-beam zone refining in ultrahigh vacuum.

They had the geometric form of cylinders of 1 mm diameter and about 8 mm length. The dHvA effect was measured using low-frequency field-modulation techniques[12] in fields up to 53 kG and temperatures as low as 0.96°K. Since nickel is ferromagnetic, the dHvA effect is periodic in $B^{-1}=[H+4\pi(1-D)M_S]^{-1}$ instead of H^{-1} as found for a normal metal.[13] The primary limitations on the accuracy with which the dHvA frequencies F can be deduced from the data arise from the uncertainty of the demagnetization factor D. In one experiment we used an as-zone-refined single-crystal cylinder 3 mm in diameter and 50 mm long. The magnetic field $\vec{H}$ was placed along the cylinder axis which nearly coincided with the [111] crystallographic direction. In this particular case, we found that the dHvA oscillations were strictly periodic in B^{-1} provided that $4\pi M_S = 6.4 \pm 0.2$ kG. The uncertainty in this measurement results solely from the uncertainty in D.

When $\vec{H}$ is tilted away from the cylinder axis, the demagnetizing field adds a further complication to the data analysis; it competes with $\vec{H}$ in the alignment of $\vec{B}$. Thus one must calculate the angle of deviation between $\vec{H}$ and $\vec{B}$ in order to assign the reduced dHvA frequency to its proper angular position with respect to the crystallographic axes. We corrected for the effect of D by assuming that the specimens were ellipsoids of revolution and then used the approximate functional form given by Gold.[14] The resulting dHvA frequencies which were obtained in this experiment are accurate in magnitude to ±2% and are located in angle with respect to the crystallographic axes to ±2°. These frequencies were converted into corresponding extremal cross-sectional areas of the Fermi surface in k space by A (in a.u.) $= 2.673 \times 10^{-9} F$ (in G).

Figure 1 shows the variation with angle of the measured extremal cross sections of two sheets of the nickel Fermi surface in the (001) and $(1\bar{1}0)$ planes. The λ_1 branch was previously measured by JT.[11] The crosses show their data points. The solid dots show some of the data points obtained in this experiment. These are shown here for comparison. Of the two sets, the JT data should be the more reliable since they used a sample geometry for which $D=0$ (a thin cylindrical disk with $\vec{H}$ in the plane of the disk).[11] The excellent agreement between the two sets of data gives us some confidence that our corrections for D are right.

When $\vec{H}$ was parallel to [111] we observed the λ_1 dHvA oscillations in fields as low as

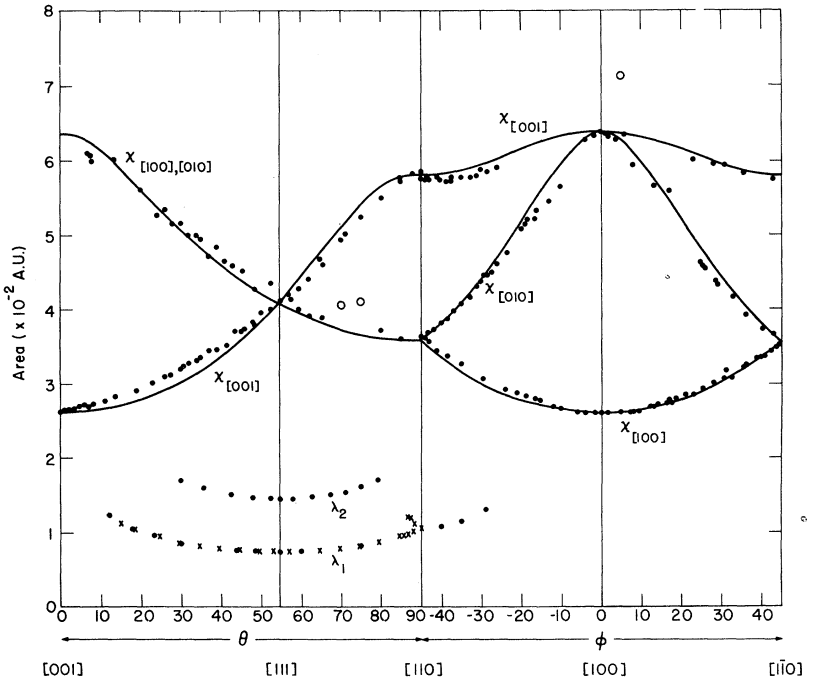

FIG. 1. The angular variation of the dHvA extremal cross-sectional area branches in the $(1\bar{1}0)$ and (001) planes of nickel. The solid curve shows the corresponding areas for the model Fermi surface represented by Eq. (1).

2 kG. The effective cyclotron mass, m^*, of the λ_1 oscillations for this orientation of $\vec{H}$ was determined from the variation of the dHvA amplitude with temperature. The value obtained, $m^* = 0.26 \pm 0.02$, agrees very well with the JT value. The Dingle scattering temperature T_D for the λ_1 oscillations was estimated from the variation of the dHvA amplitude with H. The value obtained for this is $T_D \lesssim 0.5^\circ$K.

The λ_2 branch is the second harmonic of the λ_1 branch. The dHvA oscillations arising from these two branches were phase-locked over the entire field range in which they could be simultaneously observed. The effective mass of the λ_2 branch for $\vec{H}$ parallel to [111] was found to be 0.50 ± 0.05 in agreement with that which one would expect for the second harmonic branch of λ_1.

The complex of dHvA branches labeled $\chi_{\vec{G}}$ measures the extremal cross section of three equivalent closed sheets of the Fermi surface. The angular variation of the data points in the $(1\bar{1}0)$ and (001) planes show that these sheets of the Fermi surface are very nearly ellipsoids of revolution centered on the symmetry point X of the first Brillouin zone for the face-centered-cubic lattice. The major axis of one of these ellipsoids is oriented along the appropriate ΓX zone line passing through the point X on which it is centered. The subscripts $\vec{G}$ label the direction of the major axis of the particular Fermi-surface sheet associated with the extremal cross-sectional area branch $\chi_{\vec{G}}$ in Fig. 1. The effective cyclotron masses measured from the temperature dependence of the dHvA amplitude at various points on these branches are listed in Table I.

The solid curves which are shown in Fig. 1 show the variation of the extremal cross-sectional area of a parametrized model Fermi surface which was generated in order to allow the conversion of the dHvA area branches into Fermi-surface calipers. The model which is consistent with the symmetry at X is given by

$$k = \left[\frac{k_\varphi^{\,2} k_z^{\,2}}{k_z^{\,2} + (k_\varphi^{\,2} - k_z^{\,2})\cos^2\theta}\right]^{\frac{1}{2}} + k_2 \cos 2\theta,$$

$$k\varphi = k_0 + k_4 \cos 4\varphi, \qquad (1)$$

where k is the length of the k vector from X to a point on the Fermi surface specified by the usual polar coordinates (θ, φ) choosing XW, [100] and $X\Gamma$, [001] as x and z axes, respectively. The values of the parameters which were used to obtain the curves shown in Fig. 1 are listed in Table I as well as the resultant Fermi-surface radii measured from X in three of the principal crystal directions.

Note that on setting $k_2 = k_4 = 0$, Eq. (1) represents an ellipsoid of revolution about k_z. The values of k_2 and k_4 listed in Table I are small compared with k_z and k_0, respectively. Thus, a simple quadratic band expansion was used to estimate the Fermi energy of this piece of the Fermi surface assuming that the measured cyclotron masses are good measurements of the actual band-structure masses. The value which was obtained (0.008 ± 0.001 Ry) differs from the actual Fermi energy by a scale factor dependent on the many-body mass-enhancement effects (electron-electron, electron-phonon, electron-magnon) which we have insufficient information to estimate. This scale factor may be as large as 2.

Figure 2 shows a schematic band structure which is representative of those recently proposed.[1-5] The λ_1 dHvA branch has been previously assigned[11] to the $L_2'^{\uparrow}$ neck in the copperlike sheet of the Fermi surface centered on $\Gamma_{12}^{\uparrow}$. Only the $X_2^{\downarrow}$ and $X_5^{\downarrow}$ pockets of this model have the symmetry appropriate to fit the χ dHvA branches shown in Fig. 1. The $X_5^{\downarrow}$ pocket is required by the model; the $X_2^{\downarrow}$ pocket has a doubtful existence in the model. An $X_2^{\downarrow}$ pocket would have effective cyclotron masses which would be at least twice as large as those expected for the $X_5^{\downarrow}$ pocket. If the two bands yielded Fermi-surface sheets which were about the same size, we would be forced to conclude that the χ dHvA branches arose from the $X_5^{\downarrow}$ pocket.

No evidence for another X-centered pocket was obtained in our dHvA investigation. When

Table I. Parameters of $X_5^{\downarrow}$ hole pocket (in a.u.).

$m_{[001]}^*(\theta = 0^\circ) = m_{[100]}^*(\varphi = 0^\circ) = 1.0 \pm 0.1$	
$m_{[100],\,[010]}^*(\theta = 7^\circ) = 1.9 \pm 0.2$	
$m_{[001]}^*(\varphi = \pm 45^\circ) = 1.4 \pm 0.3$	
$k_0 = 0.096\,65$	$k_z = 0.194\,34$
$k_4 = 0.004\,64$	$k_2 = 0.005\,39$
$k_{X\Gamma} = 0.200$	
$k_{XW} = 0.096$	
$k_{XU} = 0.086$	
$n_h = 0.0067$ holes/atom	
$E_F(X_5) = 0.008 \pm 0.001$ Ry	

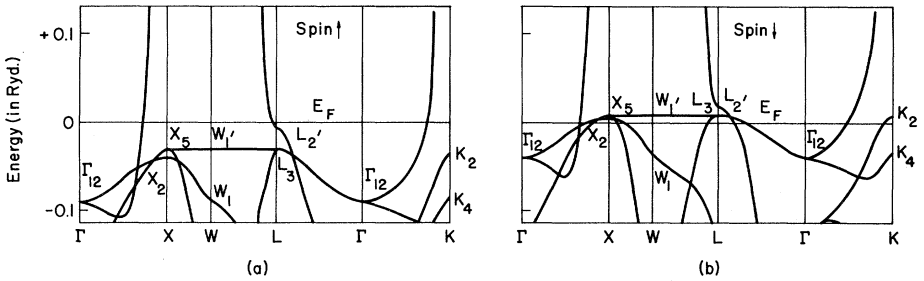

FIG. 2. Schematic band structure for ferromagnetic nickel. The spin-up (↑) bands are assumed to have lower energy.

$\vec{H}$ was along [001], the signal-to-noise ratio was high enough to allow the detection of another branch near [001] having amplitude as small as 0.05 times the amplitude of the $\chi_{[001]}$ branch. Thus if an $X_2{}^{\downarrow}$ pocket existed comparable in size to the $X_5{}^{\downarrow}$ pocket, we should have observed it even though its cyclotron mass would be at least twice as great as $X_5{}^{\downarrow}$.

If, on the other hand, we assigned the χ dHva branches to the $X_2{}^{\downarrow}$ pocket, we must conclude that the $X_5{}^{\downarrow}$ pocket is at least a factor of 2 larger in cross-sectional area than the $X_2{}^{\downarrow}$ pocket. This assignment would place $X_2{}^{\downarrow}$ about 0.01 Ry above E_F and $X_5{}^{\downarrow}$ about 0.03 Ry above E_F provided that the many-body mass-enhancement effects were negligible. If these effects were not negligible and contributed, for example, a 100% enhancement, the placements would be 0.02 and 0.06 Ry, respectively. This latter value would place the peak in the density of states associated with $X_5{}^{\downarrow}$ somewhat higher above E_F than is currently believed.

If the $X_2{}^{\downarrow}$ and $X_5{}^{\downarrow}$ levels crossed above E_F for some directions from X but not for all, we would expect to find two pockets similar in size and general shape. In this case, however, some regions of the Fermi surface of each would be representative of the low-mass $X_5{}^{\downarrow}$ level while the remaining regions would be representative of the higher mass $X_2{}^{\downarrow}$ level. This would lead to a highly anisotropic variation of the effective cyclotron mass. Our data are not conclusive on this point. However, such a crossing should lead to the appearance of another frequency near $\chi_{[001]}$ for $\vec{H}$ along [001] but as mentioned earlier this was not observed. Thus the χ dHvA branches probably arise from a pure $X_5{}^{\downarrow}$ band.

The open circles shown in Fig. 1 are data points which arise from another branch of the Fermi surface unrelated to the χ branches. The amplitude of this branch was larger than either χ branch at $\theta \simeq 75°$. It could be followed for about 5° before it became dominated by the χ branches. For $\theta \lesssim 70°$, a third branch which we suspect is the continuation of these two points was observed to beat with the $\chi_{[100],[010]}$ branch but the signal was too small to allow an accurate determination of the branch. It appeared, however, to follow the general angular variation of $\chi_{[100],[010]}$ for $\theta \lesssim 50°$. This branch then seems to have L symmetry and might be associated with the $L_3{}^{\downarrow}$ pocket. Its effective cyclotron mass could not be measured but its amplitude variation with temperature was similar to the $\chi_{[100],[010]}$ branch. If we made the admittedly unjustified and highly premature assignment of this branch to the $L_3{}^{\downarrow}$ pocket, we would find that $L_3{}^{\downarrow}$ is about 0.01 Ry above E_F.

We note in closing that the angular variation of the χ dHvA branches is very similar to the angular variation of the palladium dHvA branches which Vuillemin[15] has assigned to the X_5 light hole pocket in palladium. This seems to imply that the shape of the d bands near X_5 in these two metals must be quite similar.

---

*Work supported in part by the U. S. Army Research Office (Durham), the Alfred P. Sloan Foundation, and the Advanced Research Projects Agency.

†General Electric Predoctoral Fellow.

‡Alfred P. Sloan Research Fellow.

[1]H. Ehrenreich, H. R. Philipp, and D. J. Olechna, Phys. Rev. 131, 2469 (1963).

[2]J. C. Phillips, Phys. Rev. 133, A1020 (1964).

[3]S. Wakoh and J. Yamashita, J. Phys. Soc. Japan 19, 1342 (1964).

[4]S. Wakoh, J. Phys. Soc. Japan 20, 1894 (1965).

[5]L. Hodges and H. Ehrenreich, Phys. Letters 16, 203 (1965).

[6]J. G. Hanus, Massachusetts Institute of Technology

Solid State and Molecular Group Quarterly Progress Report No. 44, 1962 (unpublished), p. 29.
[7]J. Yamashita, M. Fukuchi, and S. Wakoh, J. Phys. Soc. Japan 18, 999 (1963).
[8]C. Kittel, Introduction to Solid State Physics (John Wiley & Sons, Inc., New York, 1956).
[9]E. Fawcett and W. A. Reed, Phys. Rev. 131, 2463 (1963).
[10]E. Fawcett and W. A. Reed, Phys. Rev. Letters 9, 336 (1962).
[11]A. S. Joseph and A. C. Thorsen, Phys. Rev. Letters 11, 554 (1963).
[12]R. W. Stark and L. R. Windmiller, to be published.
[13]J. R. Anderson and A. V. Gold, Phys. Rev. Letters 10, 277 (1963).
[14]A. V. Gold, in Proceedings of the International Conference on Magnetism, Nottingham, England, 1964 (The Institute of Physics and The Physical Society, London, 1964), p. 124.
[15]J. J. Vuillemin, Phys. Rev. 144, 396 (1966).

STRUCTURE IN THE PRECURSOR ABSORPTION IN SUPERCONDUCTING LEAD

Scott L. Norman* and David H. Douglass, Jr.†
Department of Physics and Institute for the Study of Metals, University of Chicago, Chicago, Illinois
(Received 8 August 1966)

The precursor absorption is found to consist of two peaks at 14.3 and 17 cm^{-1}, respectively. Additional structure, possibly associated with critical gaps seen in tunneling experiments, is discussed.

Previous experiments[1-4] on the far-infrared properties of superconductors have measured the superconducting energy gap by identifying it with the observed threshold for the absorption of radiation. In addition, a "precursor" absorption at energies below this threshold has been seen in Pb and Hg. The data suggested that the Pb precursor extended over a considerable energy range, with the possibility of structure within this region. In this Letter, we report the results of more detailed measurements of the absorption spectrum of bulk Pb. We find that the precursor absorption is composed of two peaks with maxima at approximately 14 and 17 cm^{-1}, respectively. In addition, we see evidence of structure on the main absorption edge which may arise from the "critical gaps" seen in superconductive tunneling.

In this experiment, we measured a quantity proportional to the surface resistance of the metal by detecting the heating of the sample due to the absorption of far-infrared radiation This direct calorimetric method has previously been employed only with superconductors whose energy gaps lay in the region accessible to microwave apparatus.[5] The arrangement of the sample within the cryostat is shown schematically in Fig. 1. Radiation generated in a diffraction-grating monochromator[6] entered the cryostat via tapered metal light pipes.[7] The sample was a piece of Pb foil 1 cm ×1 cm ×0.005 cm, and after etching appeared to be composed of approximately five crystallites; the residual resistance ratio was in excess of 3000. It was cemented to a nylon post which was in turn mounted on a Cu block in contact with the bath, and a Sb-doped Ge resistor was cemented to its back. The absorption of radiation resulted in the heating of the sample, and this temperature rise was detected as a change in the voltage appearing across the resister; the absorption of approximately 2×10^{-12} W could be detected. A second Ge resistor, mounted on an independent nylon thermal link, was exposed to the radiation and thus generated a voltage proportional to the intensity of the beam. The thermal links were selected to optimize the responses of the beam monitor and sample-thermometer combination to the mechanically chopped beam. The alternating sig-

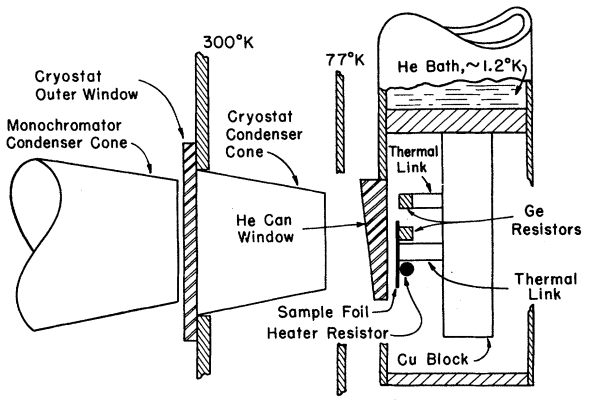

FIG. 1. Sample arrangement.